

Acceptance effect on the $N_t N_p / N_d^2$ ratio of light nuclei coalescence yields versus nucleon density fluctuations

Michael X. Zhang¹ and An Gu^{2,*}

¹*Livermore High School, Livermore, CA 94550*

²*Purdue University, West Lafayette, IN 47907*

Abstract

We employ a coalescence model to form deuterons (d), tritons (t) and helium-3 (³He) nuclei from a uniformly distributed volume of protons (p) and neutrons (n). We study the ratio $N_t N_p / N_d^2$ of light nuclei yields as a function of the neutron number fluctuations. We investigate the effect of finite transverse momentum (p_T) acceptance on the ratio, in particular, the “extrapolation factor” for the ratio as functions of the p_T spectral shape and the magnitude of neutron number fluctuations itself. The extrapolation factor is monotonic in p_T spectral “temperature parameter”, as expected, and would not cause a non-monotonic beam energy dependence of the extrapolation. The extrapolation factor is found to vary with the neutron number fluctuation magnitude and the variations are relatively small for our studied p_T ranges. More realistic simulation will be a next step to quantitatively examine whether the observed non-monotonic extrapolation factor by STAR could be explained by coalescence. Our study provides a necessary benchmark for light nuclei ratios as a probe of nucleon fluctuations, an important observable in the search for the critical point of nuclear matter.

* Corresponding author: gu180@purdue.edu

I. INTRODUCTION

Matter is comprised of quarks and gluons, the most fundamental constituents in nature together with leptons and gauge bosons. The interactions among quarks and gluons are governed by quantum chromodynamics (QCD). At low temperature and matter density quarks and gluons are confined in hadrons, while at high temperature or matter density they are deconfined in an extended volume called the quark-gluon plasma (QGP). The phase transition at low temperature and high matter density is of first order, and at high temperature and low matter density it is a smooth crossover, as predicted by lattice QCD [1]. It has been conjectured that a critical point (CP) exists on the nuclear matter phase diagram of temperature versus matter density between the first-order phase transition and the smooth crossover [2–5]. The correlation length increases dramatically near the CP causing large fluctuations of conserved quantities, such as the net-baryon number [6]. Searching for the CP is a subject of active research in heavy-ion collisions [7–15].

Light nuclei production is well modeled by nucleon coalescence [16–22]. It has been predicted by the coalescence model that large net-baryon number fluctuations affect the production rate of light nuclei [23, 24]. For example, the production of tritons (t) would be enhanced relative to that of deuterons (d) when there are extra fluctuations in the neutron density because a triton contains two neutrons (n) whereas a deuteron contains only one. As a result, the compound ratio of $N_t N_p / N_d^2$ involving the multiplicities of protons (N_p), deuterons (N_d) and tritons (N_t) would be enhanced. Similarly for the production of helium-3 (^3He) and the ratio of $N_{^3\text{He}} N_n / N_d^2$ with respect to extra fluctuations in the proton density.

Following Ref. [23–25], the deuteron average multiplicity density in the coalescence model is given by

$$\bar{n}_d / \left(\frac{3}{\sqrt{2}} A \right) = \langle (\bar{n}_p + \delta n_p)(\bar{n}_n + \delta n_n) \rangle = \bar{n}_p \bar{n}_n + \langle \delta n_p \delta n_n \rangle = \bar{n}_p \bar{n}_n (1 + (\alpha \Delta n_n)_d), \quad (1)$$

where the protons and neutrons are assumed to be at thermal equilibrium with an effective temperature T_{eff} and $A = \left(\frac{2\pi}{m_N T_{\text{eff}}} \right)^{3/2}$ is a shorthand notation (m_N is nucleon mass). Here and henceforth, \bar{n} stands for average density. The neutron density fluctuations are denoted by

$$\Delta n_n = \langle (\delta n_n)^2 \rangle / \bar{n}_n^2, \quad (2)$$

and $\alpha = \frac{\langle \delta n_p \delta n_n \rangle}{\bar{n}_p \bar{n}_n} / \Delta n_n = \frac{\bar{n}_n}{\bar{n}_p} \frac{\langle \delta n_p \delta n_n \rangle}{\langle (\delta n_n)^2 \rangle}$ denotes the correlations between proton and neutron number fluctuations. If proton and neutron numbers fluctuate independently, then $\alpha = 0$; if they fluctuate together, then $\alpha = 1$. It is noteworthy at this point that we have neglected details of deuteron formation which is determined by the deuteron wavefunction and often implemented by the Wigner function formalism (see below). Fluctuations that matter for deuteron formation are those within typical volumes of the size of the deuteron. We note this in Eq. (1) by the subscript ‘d’ in $(\alpha \Delta n_n)_d$ to indicate that it is the average $\alpha \Delta n_n$ within the typical deuteron size that is relevant.

Similarly, the triton average multiplicity density is given by

$$\bar{n}_t / \left(\frac{3\sqrt{3}}{4} A^2 \right) = \langle (\bar{n}_p + \delta n_p)(\bar{n}_n + \delta n_n)^2 \rangle = \bar{n}_p \bar{n}_n^2 (1 + (\Delta n_n)_t + 2(\alpha \Delta n_n)_t + (\beta \Delta n'_n)_t), \quad (3)$$

where $\Delta n'_n = \langle (\delta n_n)^3 \rangle / \bar{n}_n^3$ and $\beta = \frac{\langle \delta n_p (\delta n_n)^2 \rangle}{\bar{n}_p \bar{n}_n^2} / \Delta n'_n = \frac{\bar{n}_n}{\bar{n}_p} \frac{\langle \delta n_p (\delta n_n)^2 \rangle}{\langle (\delta n_n)^3 \rangle}$. Similar to the α in Eq. (1), the β parameters denotes three-body correlations. When proton and neutron numbers fluctuate independently, then $\beta = 0$; when they fluctuate together, then $\beta = 1$. The subscript ‘t’ in Eq. (3) likewise indicates that only those fluctuations averaged within the typical volume of the triton size matter. Note that in Eq. (3) we simply wrote n_n^2 for neutron pair density, however, for identical particles pair multiplicity is $N(N-1)$, so the pair fluctuations of Eq. (2) should be understood as those beyond Poisson fluctuations.

The compound ratio is thus given by

$$\frac{N_p N_t}{N_d^2} = \frac{\bar{n}_p \bar{n}_t}{\bar{n}_d^2} = \frac{1 + (\Delta n_n)_t + 2(\alpha \Delta n_n)_t + (\beta \Delta n'_n)_t}{2\sqrt{3}(1 + (\alpha \Delta n_n)_d)^2}. \quad (4)$$

If one neglects α and β , then Eq. (4) reduces to

$$\frac{N_p N_t}{N_d^2} \approx \frac{1}{2\sqrt{3}} (1 + (\Delta n_n)_t), \quad (5)$$

as in Ref. [23, 24]. Note that the factor $1/2\sqrt{3}$ comes from the thermal equilibrium assumption of nucleon abundances. The $N_t N_p / N_d^2$ ratio may therefore be a good measure of the neutron density fluctuations, a large value of which could signal critical fluctuations.

A unique signature of the CP would be a non-monotonic behavior of the ratio $N_t N_p / N_d^2$ in beam energy, where a peak of the ratio in a localized region of beam energy could signal large neutron fluctuations and the CP [23, 24]. The STAR experiment at

RHIC has recently indeed observed a non-monotonic behavior of the $N_t N_p / N_d^2$ ratio in top 10% central Au+Au collisions as a function of the nucleon-nucleon center-of-mass energy ($\sqrt{s_{NN}}$) in their Beam Energy Scan (BES) data [26]. The non-monotonic bump is observed in the ratio localized in the energy region $\sqrt{s_{NN}} = 20\text{--}30$ GeV. It is noted that the local bump is prominent in the $N_t N_p / N_d^2$ ratio of the extrapolated yields to all transverse momenta (p_T), but not as prominent in the measured fiducial range of $0.5 < p_T/A < 1.0$ GeV/ c and $0.4 < p_T/A < 1.2$ GeV/ c (where A is the mass number corresponding to each light nucleus in the ratio) [26].

In this paper, we use a toy model to generate nucleons and form d, t, and ^3He using a coalescence model. We study the ratios of the light nuclei yields as functions of the magnitude of neutron multiplicity fluctuations, and examine the role the p_T acceptance plays in those ratios.

II. COALESCENCE MODEL

The probability to form a composite particle from particle 1 at position \vec{r}_1 and with momentum \vec{p}_1 and particle 2 at position \vec{r}_2 and with momentum \vec{p}_2 is estimated by the Wigner function,

$$W(\vec{r}_1, \vec{p}_1, \vec{r}_2, \vec{p}_2) = g \cdot 8 \exp\left(-\frac{r_{12}^2}{\sigma_r^2} - \frac{p_{12}^2}{\sigma_p^2}\right), \quad (6)$$

where

$$r_{12} = |\vec{r}_1 - \vec{r}_2|, \\ p_{12} = \mu \left| \frac{\vec{p}_1}{m_1} - \frac{\vec{p}_2}{m_2} \right|,$$

and $\mu = \frac{m_1 m_2}{m_1 + m_2}$ is the reduced mass of the two-body system. The parameter σ_r is the characteristic coalescence size in configuration space and $\sigma_p = 1/\sigma_r$ (where $\hbar = c = 1$) is that in momentum space.

From the Wigner function of Eq. (6), the root mean square (RMS) radius of the coalesced composite particle can be calculated as $R = \frac{\sqrt{3m_1 m_2/2}}{m_1 + m_2} \sigma_r$. The coalescence parameter σ_r can therefore be determined by the particle size as

$$\sigma_r = \frac{m_1 + m_2}{\sqrt{3m_1 m_2/2}} R. \quad (7)$$

The deuteron is coalsced by a proton and a neutron. The RMS size of the deuteron is $R_d = 1.96$ fm [27], so for deuteron $\sigma_r = \sqrt{\frac{8}{3}} R_d = 3.20$ fm. The triton (helium-3)

is formed by coalescence between a deuteron and a neutron (proton), following the same prescription of Eq. (6). The triton RMS size is $R_t = 1.59$ fm [27], so for triton $\sigma_r = \sqrt{3}R_t = 2.75$ fm. For ${}^3\text{He}$ we also take $\sigma_r = 2.75$ fm to be symmetric in our study.

The g -factor represents the probability to have the total spin of the composite particle,

$$g = (2S + 1)/\prod_{i=1}^2 (2s_i + 1) , \quad (8)$$

where S is the spin of the composite particle (1 for d, 1/2 for both t and ${}^3\text{He}$), s_i is the spin of each coalescing particle. For d formed from p and n, the g -factor is 3/4. For t (${}^3\text{He}$) formed from d and n (p), it is 1/3.

III. SIMULATION DETAILS

We generate a system of nucleons with a toy model. The nucleons are assumed to be uniformly distributed in a cylinder of 10 fm length and 10 fm radius. The transverse momentum spectra of the nucleons are assumed to be

$$dN/dp_T \propto p_T \exp(-p_T/T) , \quad (9)$$

where the “temperature” parameter is set to $T = 150$ MeV. Note that Eq. (9) is not a thermal distribution for massive particles; we use the term “temperature” for convenience. The azimuthal angle of the momentum vector is uniformly distributed between 0 and 2π . The pseudorapidity η is assumed to be uniform between -1 and 1 . Whether to use rapidity or pseudorapidity is insignificant.

In this study, we do not use the thermal model to predict the average multiplicity, but rather set the average numbers of protons and neutrons both to $\bar{N}_p = \bar{N}_n = 20$. This is simply for convenience since our goal is only to study the effect of neutron multiplicity fluctuations. The baseline of the $N_t N_p / N_d^2$ is therefore not the $1/2\sqrt{3}$, but rather is determined by the ratio of the degeneracy g factors as $\frac{1}{3} \cdot \frac{3}{4} / (\frac{3}{4})^2 = \frac{4}{9}$ [28].

We assign Poisson fluctuations to the number of protons, and only vary the fluctuation magnitude for the number of neutrons (and focus on the compound ratio of $N_t N_p / N_d^2$). The latter is achieved by negative binomial distributions, $P(N_n = k) = C_k^{k+r-1} (1-p)^k p^r$, where r and p are free parameters. The mean and variance are $\bar{N}_n = \frac{r(1-p)}{p}$ and $\sigma_{N_n}^2 = \frac{r(1-p)}{p^2}$, respectively. The fluctuation magnitude is given by

$\sigma_{N_n}^2 = \bar{N}_n/p \equiv \theta \bar{N}_n$ (where $\theta \equiv 1/p \geq 1$), which is always larger than Poisson fluctuations unless the probability $p = 1$ when the negative binomial distribution reduces to Poisson. We use p to control the magnitude of fluctuations in N_n and choose the proper r value to have the desired average neutron multiplicity \bar{N}_n .

It is worthy to note that we utilize fluctuations in the total number of neutrons N_n event-by-event to mimic fluctuations in the local neutron number density. The purpose of our study is to investigate the behavior of $N_t N_p / N_d^2$ as a function of the neutron density fluctuation magnitude, but not to suggest that density fluctuations must be caused by fluctuations in the total multiplicity. In our simulation, given a total N_n in an event, neutrons are randomly distributed in the cylinder volume. Fluctuations in N_n thus determines the magnitude of neutron density fluctuations which is an average over the entire volume. In other words, the Δn_n in Eq. (2) can be quantified by the fluctuations in N_n beyond Poisson,

$$\Delta n_n = (\sigma_{N_n}^2 / \bar{N}_n - 1) / \bar{N}_n \equiv (\theta - 1) / \bar{N}_n. \quad (10)$$

Note that θ quantifies the fluctuations in N_n in the unit of Poisson fluctuations and $\theta - 1$ quantifies that beyond Poisson fluctuations.

A total of 1.6×10^8 events are simulated. Deuterons, tritons, and helium-3 are formed by coalescence. For each event, deuteron formation is first considered via double loops over protons and neutrons. For each deuteron, the formation of t and ^3He are implemented by looping over the remaining nucleons. The nucleons have been reordered randomly so the probabilities to form t and ^3He are unbiased. A random number uniformly distributed between 0 and 1 is used to determine whether two particles coalesce into a light nucleus or not. If the random number is smaller than the Wigner function value in consideration, then the corresponding light nucleus is formed. Once a light nucleus is formed, the coalescing particles are removed from further consideration for coalescence.

IV. RESULTS AND DISCUSSIONS

Figure 1 shows the p_T spectra of the generated neutrons and the coalesced d, t, and ^3He in the left panel, and in the right panel those spectra in the scaled p_T/A . No extra fluctuations are included beyond Poisson in this figure so the proton spectrum

is identical to that of neutrons. In the right panel, the product of the proton and neutron spectra and that of the proton and squared neutron spectra are shown in the smooth histograms. Those products would be the corresponding d and t spectra if the coalescence parameters $\sigma_p = 0$ and $\sigma_r = \infty$ in Eq. (6). The coalesced d and t spectra are steeper than the products because of the finite σ_p and σ_r in the coalescence model.

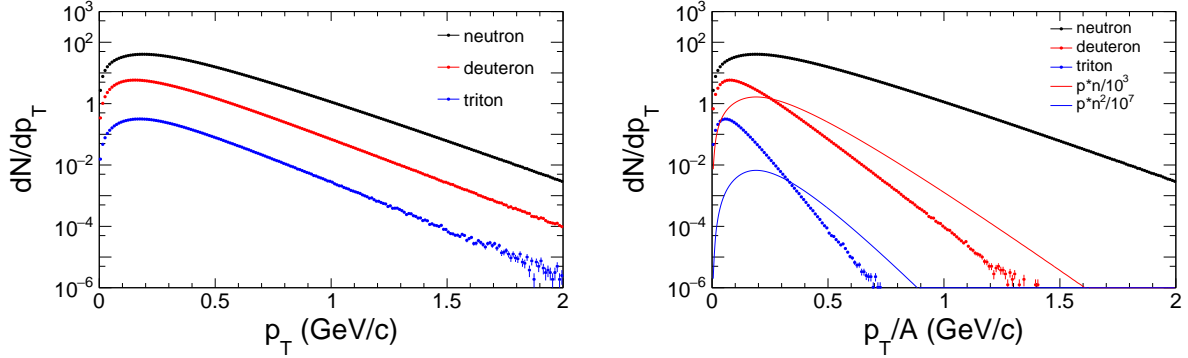


FIG. 1. (Left) Transverse momentum p_T spectra of deuteron and triton calculated by the coalescence model from a system of average $\bar{N}_p = 20$ protons and $\bar{N}_n = 20$ neutrons at “temperature” $T = 150$ MeV randomly distributed within a cylinder of 10 fm radius and 10 fm length. No extra fluctuations are included beyond Poisson. (Right) The same spectra plotted as function of p_T/A (A is the corresponding mass number). Superimposed in curves are the products of $(dN_p/dp_T) \times (dN_n/dp_T)$ and $(dN_p/dp_T) \times (dN_n/dp_T)^2$ at the same p_T/A value, arbitrarily scaled to compare to the shapes of the deuteron and triton spectra, respectively.

Figure 2 shows in the left panel the yield ratios of N_d/N_p and N_t/N_d as functions of the neutron fluctuation magnitude $\Delta n_n = (\sigma_{N_n}^2/\bar{N}_n - 1)/\bar{N}_n \equiv (\theta - 1)/\bar{N}_n$. The N_t/N_d ratio increases with Δn_n , consistent with the expected stronger effect of neutron density fluctuations on t than on d production. The N_d/N_p ratio decreases slightly but statistically significant. This is counter-intuitive as one would expect no dependence because \bar{N}_n is the same for all values of Δn_n ; the events with more neutrons would be balanced out by those with fewer neutrons in terms of deuteron production. However, $\bar{N}_p = 20$ is fixed and fluctuations in N_p are treated uncorrelated to those in N_n in our study. The production of deuterons will be “saturated” in events with large N_n and would not get “equal” share of deuteron production. As a result, the N_d/N_p is smaller for larger Δn_n .

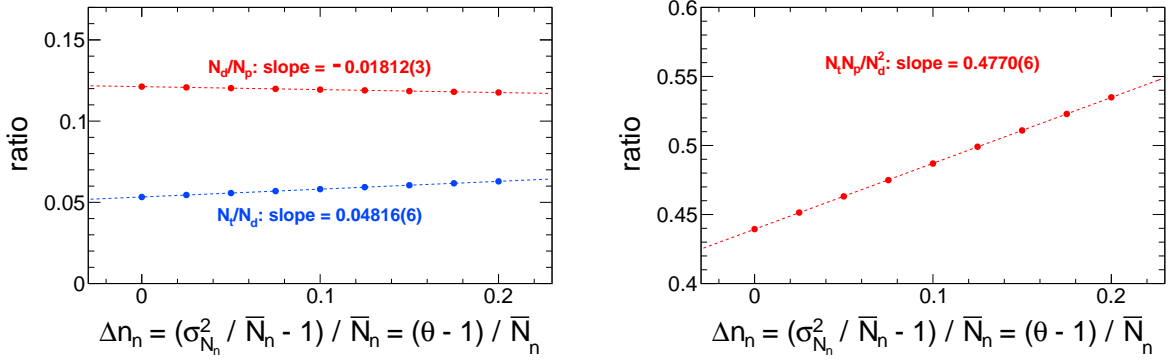


FIG. 2. Yield ratios of N_d/N_p and N_t/N_d (left) and $N_t N_p / N_d^2$ (right) as functions of $\Delta n_n = (\sigma_{N_n}^2 / \bar{N}_n - 1) / \bar{N}_n \equiv (\theta - 1) / \bar{N}_n$, the magnitude of neutron multiplicity fluctuations beyond Poisson. The light nuclei are formed by coalescence from a system of average $\bar{N}_p = 20$ protons and $\bar{N}_n = 20$ neutrons at $T = 150$ MeV randomly distributed within a cylinder of 10 fm radius and 10 fm length.

Figure 2 right panel shows the $N_t N_p / N_d^2$ ratio as function of $\Delta n_n = (\sigma_{N_n}^2 / \bar{N}_n - 1) / \bar{N}_n \equiv (\theta - 1) / \bar{N}_n$. The $N_t N_p / N_d^2$ clearly increases with Δn_n . The slope is about 0.477, significantly non-zero, and the intercept is about 0.439. These values are roughly equal to the expected degeneracy factor $4/9$. The slight deviations may be due to the different size parameters for deuteron and triton.

The measured non-monotonic feature of the $N_t N_p / N_d^2$ ratio as a function of beam energy $\sqrt{s_{NN}}$ by STAR appears to depend on the considered p_T/A range [26]; the non-monotonic feature is stronger for the extrapolated yield ratio than for those in the limited p_T/A acceptance. This is shown in the left panel of Fig. 3 where the STAR measured $N_t N_p / N_d^2$ ratios from the total extrapolated yields and from two measured p_T/A ranges are reproduced. The non-monotonic behavior around $\sqrt{s_{NN}} = 20\text{--}30$ GeV is prominent in the total yield ratio but not as prominent in the ratios from the measured p_T ranges. The “extrapolation factor”, i.e., the $N_t N_p / N_d^2$ ratio of the total light nuclei yields extrapolated to the entire p_T/A range $[0\text{--}\infty)$ divided by the ratio of those measured within a fiducial p_T/A range, is shown in the right panel of Fig. 3 for the two measured p_T/A ranges. The statistical uncertainties between the fiducial yield of a given p_T spectrum and the extrapolated total yield are correlated, so are the systematic uncertainties. Thus, the statistical and systematic uncertainties are taken to be the quadratic *difference* of the corresponding uncertainties on the $N_t N_p / N_d^2$ ratio between

the fiducial p_T/A range and the total range. As expected, the extrapolation factors are peaked at the $\sqrt{s_{NN}} = 20\text{--}30$ GeV range and are non-monotonic. The non-monotonic effect is on the order of 10%.

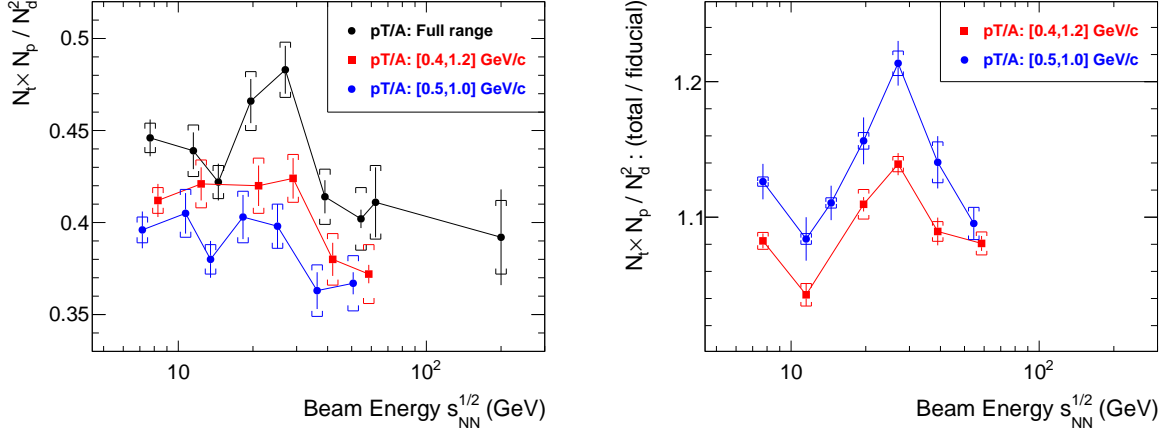


FIG. 3. (Left) The $N_t N_p / N_d^2$ ratio as functions of beam energy $\sqrt{s_{NN}}$ measured by STAR. The ratio of the extrapolated total yields and those from two measured p_T/A ranges are shown. The ratios from the measured p_T/A ranges are shifted in the horizontal axis for clarity. (Right) The acceptance factor, i.e., the $N_t N_p / N_d^2$ ratio from the extrapolated total yields divided by that from the fiducial yields in the given measured p_T/A range, is shown for the two measured p_T/A ranges as function of $\sqrt{s_{NN}}$. The statistical and systematic uncertainties on the extrapolation factor are the quadratic *difference* of the corresponding uncertainties of the $N_t N_p / N_d^2$ ratio between the given measured p_T/A range and the total range. The rightmost square is shifted in the horizontal axis for clarity.

It is, therefore, important to investigate whether a non-monotonic extrapolation factor can result from trivial physics. To this end, we first examine the $N_t N_p / N_d^2$ ratio as function of p_T/A in our toy-model simulation. This is shown in Fig. 4 left panel for various θ values. The falling and rising characteristic of the shape is determined by the p_T distribution of Eq. (9). The shapes are similar for the various fluctuation magnitudes and the overall ratio increases with θ as expected. The right panel of Fig. 4 shows the extrapolation factor as a function of Δn_n . (Note that the total yields in simulation are known of course, not from extrapolation, but we keep use of the term “extrapolation factor”.) Two fiducial ranges are depicted, $p_T/A = 0.1\text{--}0.2$ and $0.3\text{--}0.4$ GeV/c. The extrapolation factor varies with Δn_n ; however, the variation is relatively small, about

1% for the $p_T/A = 0.3\text{--}0.4$ GeV/ c range for $\theta = 2$, a fluctuation magnitude of a factor of 2 of that of Poisson fluctuations. Note that we have examined only relatively narrow p_T/A ranges at small p_T/A values because of statistics considerations. The fiducial p_T/A ranges in the STAR analysis are relatively large and wide, so no direct comparisons can be made between our study and the STAR results. Such comparisons will require more realistic simulations which we leave to a future work.

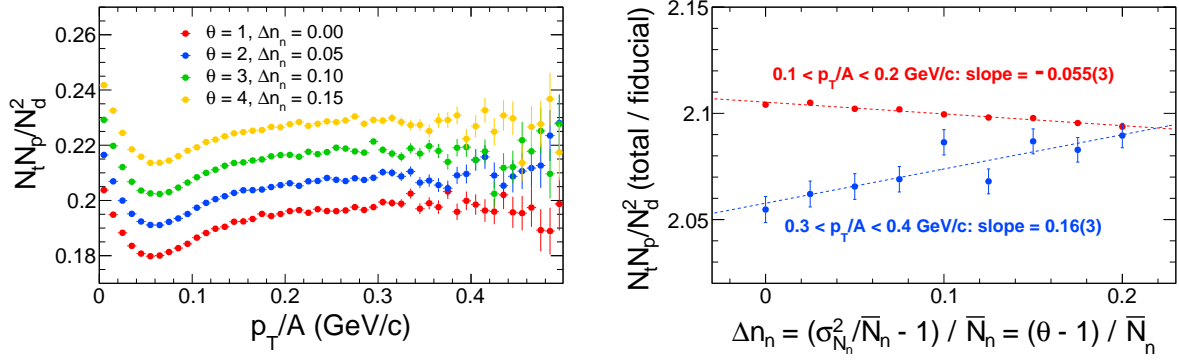


FIG. 4. (Left) The $N_t N_p / N_d^2$ ratio as functions of p_T/A . (Right) The $N_t N_p / N_d^2$ “extrapolation factor” from $p_T/A = 0.1\text{--}0.2$ and $0.3\text{--}0.4$ GeV/ c as a function of $(\sigma_{N_n}^2 / \bar{N}_n - 1) / \bar{N}_n$. The light nuclei are formed by coalescence from a system of average $\bar{N}_p = 20$ protons and $\bar{N}_n = 20$ neutrons at $T = 150$ MeV randomly distributed within a cylinder of 10 fm radius and 10 fm length.

In heavy ion collisions, the p_T distributions can be significantly altered by collective radial flow. The shape of the p_T distributions affects the $N_t N_p / N_d^2$ ratio as function of p_T/A . For convenience, we vary the T parameter of Eq. (9) in our simulation to investigate the effect of the nucleon p_T spectral shape on the extrapolation factor for the $N_t N_p / N_d^2$ ratio. Figure 5 shows the T dependence of the extrapolation factor for $p_T/A = 0.3\text{--}0.4$ GeV/ c , with a given neutron fluctuation value $\Delta n_n = (\sigma_{N_n}^2 / \bar{N}_n - 1) / \bar{N}_n = 0.1$ (i.e., $\theta = 3$). The extrapolation factor varies with T as expected, but the variations are monotonic. Thus, the T -dependent p_T spectral shape would not cause a non-monotonic $N_t N_p / N_d^2$ enhancement from limited to full acceptance in any given localized T range.

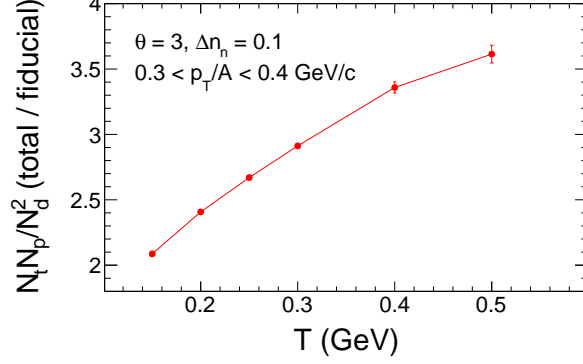


FIG. 5. The $N_t N_p / N_d^2$ “extrapolation factor” for the $p_T/A = 0.3\text{--}0.4$ GeV/ c acceptance as a function of T , with $\theta = 3$ or $\Delta n_n = (\sigma_{N_n}^2 / \bar{N}_n - 1) / \bar{N}_n = 0.1$. The light nuclei are formed by coalescence from a system of average $\bar{N}_p = 20$ protons and $\bar{N}_n = 20$ neutrons randomly distributed within a cylinder of 10 fm radius and 10 fm length.

V. SUMMARY

We have simulated light nuclei production with the coalescence model from a system of nucleons with varying magnitude of nucleon multiplicity fluctuations, $(\sigma_{N_n}^2 / \bar{N}_n - 1) / \bar{N}_n$. It is found that the light nuclei yield ratio $N_t N_p / N_d^2$ increases linearly with $(\sigma_{N_n}^2 / \bar{N}_n - 1) / \bar{N}_n$, confirming the finding in Ref. [23, 24]. We have further investigated the effect of finite acceptance by studying the “extrapolation factor” for the $N_t N_p / N_d^2$ ratio as a function of $(\sigma_{N_n}^2 / \bar{N}_n - 1) / \bar{N}_n$ and the p_T spectra parameter T . The extrapolation factor is found to be monotonic as a function of T as expected. The extrapolation factor is found to vary with $(\sigma_{N_n}^2 / \bar{N}_n - 1) / \bar{N}_n$, and the variations are found to depend on the fiducial p_T/A range.

Our study provides a necessary benchmark for light nuclei ratios as a probe of nucleon fluctuations, an important observable in the search for the critical point of nuclear matter. More realistic simulations are called for in order to make quantitative comparisons to the STAR results and infer physics implications from the observed non-monotonic $N_t N_p / N_d^2$ ratio as function of beam energy, as we outline below.

We have only simulated a system of nucleons within a fixed cylindrical volume and used a slope parameter to vary the p_T distribution. In relativistic heavy ion collisions the system is more reasonably described by local thermal equilibrium with a collective radial flow velocity field. In fact, one can perform a more realistic simulation by gen-

erating a thermal system of nucleons and other hadrons with a Gaussian (rather than uniform) density source and boost the hadrons with a radial velocity field. The thermal temperature, the net-baryon chemical potential, the collective radial velocity, and the total charged hadron multiplicity (which fixes the volume) can readily be obtained from experimental measurements at various beam energies. One can then calculate the $N_t N_p / N_d^2$ ratio by the coalescence model to mimic the STAR data as a function of beam energy and examine what magnitude of the neutron density fluctuations the STAR data entail and what the observed acceptance effect implies. In addition, we have assumed in the present study that the fluctuations in the numbers of protons and neutrons are independent. One may implement varying degrees of correlations between these fluctuations and study the effect on the $N_t N_p / N_d^2$ ratio. We leave these improved studies to a future work.

ACKNOWLEDGEMENT

We thank Dr. Fuqiang Wang for suggesting the project and for many fruitful discussions. This work was supported in part by the U.S. Department of Energy (Grant No. DE-SC0012910).

-
- [1] Y. Aoki, G. Endrodi, Z. Fodor, S. D. Katz, and K. K. Szabo, [Nature](#) **443**, 675 (2006), [arXiv:hep-lat/0611014](#).
 - [2] A. M. Halasz, A. D. Jackson, R. E. Shrock, M. A. Stephanov, and J. J. M. Verbaarschot, [Phys. Rev. D](#) **58**, 096007 (1998), [arXiv:hep-ph/9804290](#).
 - [3] M. A. Stephanov, K. Rajagopal, and E. V. Shuryak, [Phys. Rev. Lett.](#) **81**, 4816 (1998), [arXiv:hep-ph/9806219](#).
 - [4] M. A. Stephanov, [Prog. Theor. Phys. Suppl.](#) **153**, 139 (2004), [arXiv:hep-ph/0402115](#).
 - [5] K. Fukushima and T. Hatsuda, [Rept. Prog. Phys.](#) **74**, 014001 (2011), [arXiv:1005.4814 \[hep-ph\]](#).
 - [6] M. A. Stephanov, [Phys. Rev. Lett.](#) **107**, 052301 (2011), [arXiv:1104.1627 \[hep-ph\]](#).
 - [7] M. M. Aggarwal *et al.* (STAR), (2010), [arXiv:1007.2613 \[nucl-ex\]](#).

- [8] L. Adamczyk *et al.* (STAR), [Phys. Rev. Lett. **112**, 032302 \(2014\)](#), [arXiv:1309.5681 \[nucl-ex\]](#).
- [9] X. Luo, [Nucl. Phys. A **956**, 75 \(2016\)](#), [arXiv:1512.09215 \[nucl-ex\]](#).
- [10] A. Bzdak, S. Esumi, V. Koch, J. Liao, M. Stephanov, and N. Xu, [Phys. Rept. **853**, 1 \(2020\)](#), [arXiv:1906.00936 \[nucl-th\]](#).
- [11] S. Acharya *et al.* (ALICE), [Phys. Lett. B **807**, 135564 \(2020\)](#), [arXiv:1910.14396 \[nucl-ex\]](#).
- [12] J. Adamczewski-Musch *et al.* (HADES), [Phys. Rev. C **102**, 024914 \(2020\)](#), [arXiv:2002.08701 \[nucl-ex\]](#).
- [13] J. Adam *et al.* (STAR), [Phys. Rev. Lett. **126**, 092301 \(2021\)](#), [arXiv:2001.02852 \[nucl-ex\]](#).
- [14] M. Abdallah *et al.* (STAR), [Phys. Rev. C **104**, 024902 \(2021\)](#), [arXiv:2101.12413 \[nucl-ex\]](#).
- [15] M. S. Abdallah *et al.* (STAR), [Phys. Rev. Lett. **128**, 202303 \(2022\)](#), [arXiv:2112.00240 \[nucl-ex\]](#).
- [16] S. T. Butler and C. A. Pearson, [Phys. Rev. **129**, 836 \(1963\)](#).
- [17] H. Sato and K. Yazaki, [Phys. Lett. B **98**, 153 \(1981\)](#).
- [18] L. P. Csernai and J. I. Kapusta, [Phys. Rept. **131**, 223 \(1986\)](#).
- [19] C. B. Dover, U. W. Heinz, E. Schnedermann, and J. Zimanyi, [Phys. Rev. C **44**, 1636 \(1991\)](#).
- [20] R. Scheibl and U. W. Heinz, [Phys. Rev. C **59**, 1585 \(1999\)](#), [arXiv:nucl-th/9809092](#).
- [21] L.-W. Chen, C. M. Ko, and B.-A. Li, [Phys. Rev. C **68**, 017601 \(2003\)](#), [arXiv:nucl-th/0302068 \[nucl-th\]](#).
- [22] Y. Oh, Z.-W. Lin, and C. M. Ko, [Phys. Rev. C **80**, 064902 \(2009\)](#), [arXiv:0910.1977 \[nucl-th\]](#).
- [23] K.-J. Sun, L.-W. Chen, C. M. Ko, and Z. Xu, [Phys. Lett. **B774**, 103 \(2017\)](#), [arXiv:1702.07620 \[nucl-th\]](#).
- [24] K.-J. Sun, L.-W. Chen, C. M. Ko, J. Pu, and Z. Xu, [Phys. Lett. B **781**, 499 \(2018\)](#), [arXiv:1801.09382 \[nucl-th\]](#).
- [25] K.-J. Sun and L.-W. Chen, [Phys. Rev. C **95**, 044905 \(2017\)](#), [arXiv:1701.01935 \[nucl-th\]](#).
- [26] M. Abdulhamid *et al.* (STAR), [Phys. Rev. Lett. **130**, 202301 \(2023\)](#), [arXiv:2209.08058 \[nucl-ex\]](#).
- [27] G. Ropke, [Phys. Rev. C **79**, 014002 \(2009\)](#), [arXiv:0810.4645 \[nucl-th\]](#).

- [28] S. Wu, K. Murase, S. Tang, and H. Song, [Phys. Rev. C **106**, 034905 \(2022\)](#), [arXiv:2205.14302 \[nucl-th\]](#).